PHYSICAL REVIEW B VOLUME 28, NUMBER 12 15 DECEMBER 1983

Melting transition of submonolayer xenon, krypton, and argon films on graphite: A computer simulation study

Farid F. Abraham
IBM Research Laboratory, San Jose, California 95193
(Received 11 July 1983)

Using the molecular dynamics simulation technique, I have studied the melting of submonolayer xenon, krypton, and argon films on graphite. I observe first-order melting of xenon which mimics the melting of an idealized two-dimensional film, first-order melting of krypton with the existence of an "incipient triple point," and continuous melting of argon over a temperature interval of approximately 7 K. The role of the graphite lateral substrate structure on the melting of these various rare-gas films is emphasized. The simulation experiments are consistent with a recent high-resolution x-ray experiment of melting by McTague *et al.* [Phys. Rev. B 25, 7765 (1982)].

In a recent x-ray scattering experiment, McTague, Als-Nielsen, Bohr, and Nielsen[1] examined the melting of xenon, krypton, and argon films on the (001) basal plane of *ZYX* graphite at submonolayer coverages and found the melting behavior to differ markedly between the various rare-gas films. Comparison of all three systems under the same experimental conditions is a significant advance in clarifying the complexities of substrate-influenced melting and provided the stimulus to carry out a similar program employing computer simulation experiments. Using the molecular dynamics simulation technique, I have studied the melting of submonolayer xenon, krypton, and argon films on graphite. I observe first-order melting of xenon which mimics the melting of an idealized two-dimensional film, first-order melting of krypton with the existence of an "incipient triple point," and continuous melting of argon over a temperature interval of approximately 7 K. All of these findings are consistent with the experiment of McTague *et al.*[1] The role of the graphite lateral substrate structure in the melting of these various rare-gas films is emphasized. Earlier simulation studies have considered the melting of near-monolayer xenon films.[2]

The details of the simulation procedure are given in Refs. 2 and 3 and will be briefly described here. The Lennard-Jones pair potential is chosen to represent the interaction between the various atoms of the rare-gas atom/graphite system. The Xe-Xe, Kr-Kr, and Ar-Ar parameters are taken to be $\epsilon/k = 236$, 170, and 120 K and $\sigma = 3.92$, 3.60, and 3.38 Å, respectively. The Xe-C, Kr-C, and Ar-C parameters are taken to be $\epsilon/k = 76.38$, 64.83, and 54.46 K and $\sigma = 3.38$, 3.22, and 3.11 Å, respectively (C denotes carbon). Simple pairwise additivity of the atomic interactions is assumed, and the carbon atoms defining the semi-infinite graphite solid are fixed at their lattice sites. In order to reduce computational time in the evaluation of forces, certain approximations and procedures are implemented. The adatoms' interaction is truncated at 3σ. Also, the "chain-link" method is employed so that the tests for locating atoms within 3σ of any particular atom need only be performed over a small subset of the total number of the adatoms.[4] The atomic positions of the graphite surface define the basal plane of the computational box, this being a parallelogram compatible with the triangular lattice of a close-packed, registered adatom crystal. Periodic boundary conditions are imposed at the four faces of the computational cell which pass through the sides of the basal parallelogram at normal incidence to the surface. The basal plane of the computational box must be compatible with the graphite structure, otherwise periodic replication creates unphysical size dependences. A reflecting wall is placed at the top of the computational box at a 9-Å height, but an adatom reaches this normal extent very infrequently at the studied temperatures. Conventional molecular dynamics is employed and consists of numerically integrating Newton's equations of motion to obtain trajectories of the atoms. Using a fifth-degree numerical integration scheme, we adopt a 0.05-psec time step. The atomic velocities are renormalized at every numerical time step so that the mean kinetic energy corresponds to the specified temperature. For equilibrium states, time averaging of the state variables over a sufficiently long interval of the temporal evolution of the system will yield proper equilibrium properties. At the lowest temperature of 0.36 (in reduced units[2,3]), the rare-gas systems's initial configuration is a two-dimensional strip spanning the x dimension with the appropriate solid-state density and with a coverage corresponding to approximately 0.6. The number of rare-gas atoms for the Xe, Kr, and Ar films are 1175, 1323, and 1680, respectively, and this corresponds to a cell dimension of approximately 200 Å. The analog to this present study, but for a two-dimensional Lennard-Jones film, is reported in Ref. 5, Figs. 16 and 17. The presentation of the simulation results will be expressed as a function of reduced temperature, since this will clearly demonstrate variations from the idealized two-dimensional picture where the film properties of the three rare-gas systems would be identical.

A series of simulations have been performed at reduced temperatures spanning the melting regime of the various films. The total simulation time for each temperature needed to be very long in the case of Ar film melting, where over 100 000 time steps were executed in order to obtain reasonable statistics. The adatom energy per atom as a function of temperature is presented in Fig. 1(a) for the Xe, Kr, and Ar films. While we note a discontinuous change in the energy at the melting temperature of 0.40 for Xe and of 0.48 for Kr, the energy variation for the Ar film is continuous (to within the experimental error) over the entire temperature region. The Xe melting temperature of 0.40 agrees very well with the two-dimensional melting temperature of 0.41. Of course, any deviation from 0.41 is a consequence

of the substrate interaction and deviation from strictly two-dimensional behavior. The deviation is especially large for the Kr and Ar films. All of the adatom energies converge to a common high-temperature fluid film trend. In Fig. 1(b), the percentage of adatoms that are commensurate with the graphite substrate is shown as a function of temperature, where commensurability is arbitrarily defined as an adatom being displaced from a graphite adsorption site by an amount that is less than two-tenths of a graphite lattice constant. Until the film melts, the Kr atoms are highly commensurate. Actually, it is the "premelted" surface atoms that are incommensurate (see Fig. 4) and all of the solid Kr atoms remain commensurate until melting; that is why the percent commensurate is not more nearly 100%. It is interesting to note that while Xe and Ar films are typically viewed as incommensurate, the Xe film is 50% "more" incommensurate than the Ar film. The commensurability decreases continuously with increasing temperature, all films converging to a common high-temperature fluid film trend. There might be a discontinuity in the Xe curve at melting, but it is small if it exists. In Fig. 2, structure factor properties as a function of temperature are presented for the various rare-gas films. Both for the peak position and the half-width at half maximum of the first Bragg peak, the temperature dependence is consistent with temperature dependence of the adatom energy for the various films. The Xe and Kr films melt by first-order transitions at their respective melting temperatures, while the Ar film melting is continuous.

The character of the melting of the various films can be best appreciated from the trajectory pictures of "typical" states of the Xe, Kr, and Ar films as a function of temperature as shown in Figs. 3 and 4. For the Xe film at $T^* = 0.38$, we see a solid strip with premelted surfaces and coexisting low-density vapor, similar to the findings for the two-dimensional Lennard-Jones simulation.[5] At $T^* = 0.4$ and greater, the film is liquid with density decreasing with increasing temperature and coexisting with a low-density vapor. Looking at Fig. 4, we note that the Kr film remains solid with premelted surfaces and coexisting vapor until a temperature of 0.48 is reached, when it becomes a homogeneous fluid. From the phase diagrams in Fig. 6 of Ref. 1, an estimate of the critical temperature gives approximately 0.48. Hence the Kr film melts in the neighborhood of the critical temperature for this system. This simulation finding is in agreement with the incipient triple-point picture of Butler *et al.*[6] It is in Fig. 3 that we note the different char-

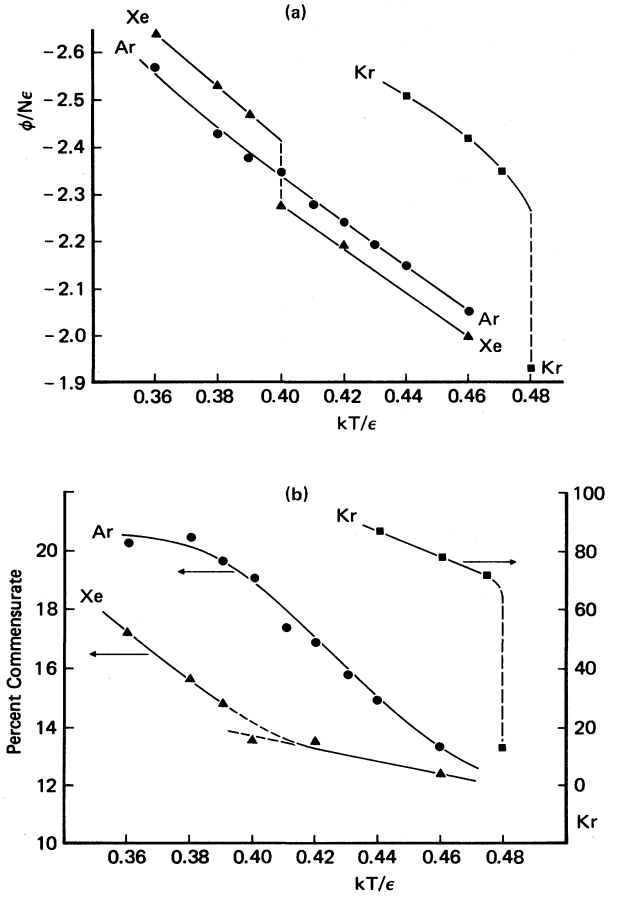

FIG. 1. Adatom energy per atom (top) and percent commensurate with respect to the graphite substrate (bottom) as a function of reduced temperature $T^* = kT/\epsilon$ for the Xe, Kr, and Ar films.

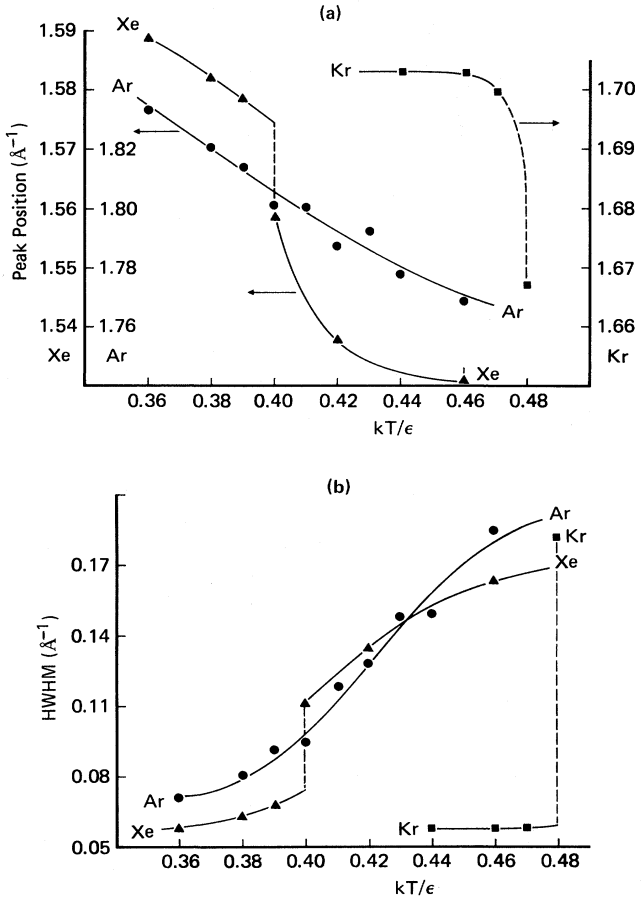

FIG. 2. Peak position (top) and half-width at half maximum (bottom) of the structure factor as a function of reduced temperature $T^* = kT/\epsilon$ for the Xe, Kr, and Ar films.

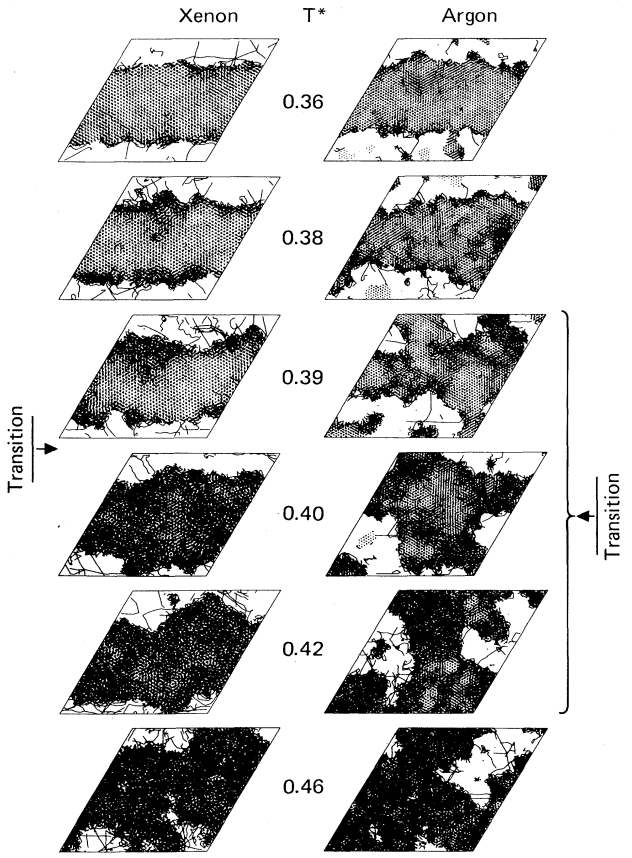

FIG. 3. Trajectory analysis of the adatom motions for the Xe and Ar films as a function of reduced temperature T^*.

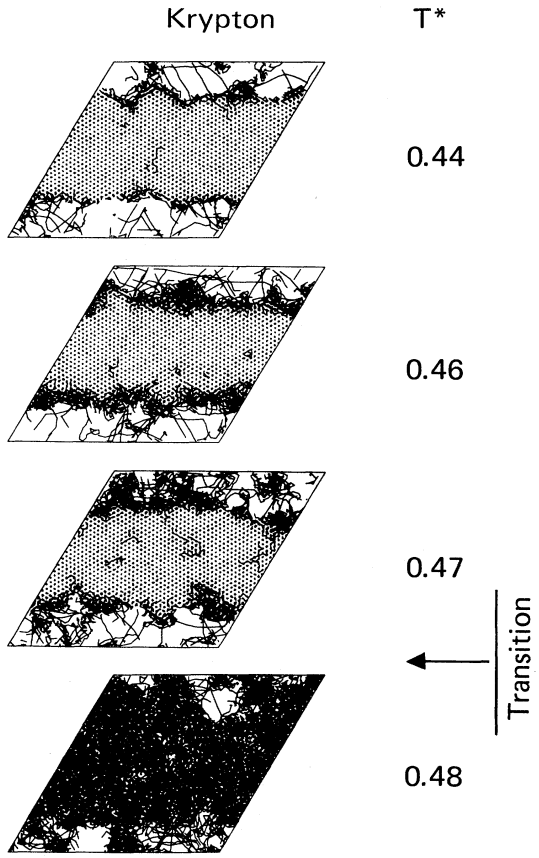

FIG. 4. Trajectory analysis of the adatom motions for the Kr film as a function of reduced temperatrue T^*.

acter of the Ar film's state as a function of temperature that suggests an explanation of the continuous nature of the melting process. Through the Ar melting regime of 0.39 to 0.44, we note an apparent coexistence of liquidlike and solidlike regions, this being shown by the atomic mobility of the respective regions in the film. With increasing temperature, the dominance of the liquidlike regions increases continuously until the film is entirely liquid around $T^* = 0.44$.

The origin of these substrate-mediated features can best be appreciated by noting the following facts. The barrier to translation of a single adatom on the graphite surface from one site to another is essentially the same for Xe, Kr, and Ar atoms and is approximately 50 K, while the melting temperatures of Xe, Kr, and Ar are 95, 82, and 47 K, respectively. Also, the reduced densities for the Xe, Kr, and Ar solid films to be commensurate with the graphite substrate are 0.978, 0.820, and 0.727, respectively, while the reduced densities for an incommensurate Lennard-Jones solid and liquid at melting are 0.83 and 0.73, respectively. Hence the incommensurate Xe solid melts to an incommensurate liquid with a lateral atomic mobility weakly influenced by the underlying substrate. For Kr, the solid density corresponds to a commensurate structure relative to the graphite substrate which provides a greater stability and, hence, a higher melting temperature. At melting, the Kr liquid is incommensurate and at a temperature comparable with the critical temperature of an incommensurate fluid; this is the origin of the incipient triple point. Also, the Kr fluid temperature is sufficiently high so that the lateral atomic mobility is weakly influenced by the underlying substrate. Ar is a further step up in the hierarchy of complexity. The incommensurate Ar solid melts to a liquid at a reduced temperature comparable with that of Xe, but the liquid Ar density is approximately that required for an Ar solid film to be commensurate with the graphite substrate. Furthermore, the lateral atomic mobility is *strongly* influenced by the underlying substrate since the melting temperature and the energy barrier between graphite sites are essentially equal. Hence the configurations of the condensed-phase Ar film upon melting are strongly influenced by its interaction with the graphite substrate, resulting in a continuous melting transition over a 7-K temperature window, and manifest a solidlike and liquidlike character in coexistence during the molecular dynamics simulation. At a sufficiently high reduced temperature, all of the liquid films converge to like properties.

ACKNOWLEDGMENT

I thank J. A. Barker for discussions and reading the manuscript.

[1]J. P. McTague, J. Als-Nielsen, J. Bohr, and M. Nielsen, Phys. Rev. B 25, 7765 (1982).
[2]S. Koch and F. F. Abraham, Phys. Rev. B 27, 2964 (1983); F. F. Abraham, Phys. Rev. Lett. 50, 978 (1983).
[3]F. F. Abraham, S. W. Koch, and W. E. Rudge, Phys. Rev. Lett. 49, 1830 (1982).
[4]R. W. Hockney and J. W. Eastwood, *Computer Simulation Using Particles* (McGraw-Hill, New York, 1981), Sec. 8-4.
[5]F. F. Abraham, Phys. Rep. 80, 339 (1981).
[6]D. M. Butler, J. A. Litzinger, G. A. Stewart, and R. B. Griffiths, Phys. Rev. Lett. 42, 1289 (1979).